Proceedings World Geothermal Congress 2000
Kyushu - Tohoku, Japan, May 28 - June 10, 2000

CORROSION RATES IN THE DEW-POINT ZONE OF SUPERHEATED STEAM

Culivicchi Giorgio, Perini Renato, Tarquini, Bruno, and Lenzi, Alessandro

ERGA, ENEL Group, Larderello Laboratory Unit, Piazza Leopolda 1, ITALY

Key Words*:* geothermal, geochemical, carbon steel, stainless steel, chloride corrosion, Larderello

ABSTRACT

The corrosion rates of carbon steel and 13% Cr stainless steel when superheated steam begins to condense on the metal surface were experimentally measured. Generalised and pitting corrosion in the geothermal fluid was monitored by weight-loss in steam-inserted cooled coupons. In these conditions, the surface is wetted by an acid film due to the hydrogen and ammonia chloride dissolution. Tests were made in several steams with chloride concentration ranging between 0 and 10 ppm. The correlation $y=0.315 \cdot [Cl]_{steam}$ has been determined as the relationship between the corrosion rate and chloride content.

1. INTRODUCTION

Corrosion in geothermal pipelines and turbines chiefly originates by chloride, present in the steam as hydrogen chloride (HCl) and ammonium chloride (NH_4Cl) (Bracaloni et al. 1995).

The chloride ion, when carried by the above-mentioned species, is formed in the presence of small amounts of condensed steam and can induce massive corrosion phenomena at high thermal dispersion points and at the turbine dew point. The condensed phase can reach very high chloride concentrations and pH values of 2 – 4, depending on the chloride content in the vapour phase. The pH in the fully condensed phase, although different owing to variations in ionic species concentration, is mainly affected by the chloride content.

Although other chemical components of geothermal fluids and their thermodynamical features can synergistically affect corrosion, chloride concentration in the steam drives most corrosion phenomena currently observed in geothermal plants.

This paper presents generalised corrosion and pitting damage results on carbon steel and 13% Cr stainless steel (AISI 403) when they were exposed to geothermal fluids with different chloride contents. The results define an empirical correlation between the corrosion rate (v_{corr}) and chloride content (C_{Cl}), extensively utilized in Italian geothermal field exploitation as a tool in the design and engineering of geothermal power plants.

2. DEW-POINT COMPOSITION

In superheated steam the dew point can be reached through isobaric or adiabatic transformations. The first process occurs by cooling in the pipelines due to inadequate thermal insulation or the presence of stagnation points. The adiabatic process is observed during steam expansion in the turbine.
Knowing the thermodynamic conditions of the fluid and the average chemical composition of steam, the first droplet composition at the dew point can be calculated and solid phase segregation phenomena can be estimated. Several calculations have been performed with a self developed software (LAVAG code) and using the thermochemical data of fluids at the Larderello geothermal field.

The effects on steam composition and dew-point parameters are reported for a run of the LAVAG code modelling the Lumiera well at Larderello. (Table 1). This table shows the chemical composition of steam and dew-point droplets for cooling at constant pressure and for adiabatic expansion assuming 80% turbine efficiency. The moisture at the dew point has low pH values of 3.8 – 3.9 and very high chloride and boric acid contents. Hydrogen chloride and ammonium chloride mainly drive the low pH values and, as expected, the pH diminishes as the chloride content increases. The ammonia content in the vapour is not sufficient to buffer the solution to neutral pH. One calculation predicted that 80 mg/kg of chloride can generate up to 9,600 and 38,700 g/kg (H_2O) of NH_4Cl for isobaric cooling and adiabatic expansion respectively. With an ammonia content of ≈ 1000 mg/kg, NH_4Cl concentration in the first drop reaches 32,600 and 203,600 g/kg (H_2O) for the same processes.

Ammonium chloride can also raise the ebullition temperature allowing condensation at higher temperatures due to the increasing in salinity. This phenomenon is almost negligible during isobaric cooling but is relatively important for adiabatic expansion.

3. MATERIALS AND METHODS

In geothermal plants carbon steel and martensitic stainless steel are usually used for pipelines and turbine materials. Both of these materials can be damaged by corrosion in the presence of condensed steam at low pH values. In the first case, we have observed general corrosion, whereas pitting phenomena arise in stainless steel.

This study has focused on the most commonly used steels in geothermal practice, i.e. carbon steel API 5 LX and AISI 403 stainless steel, normally used for turbine blades (Table. 2). Corrosion coupons of the above listed materials were prepared and directly introduced in the steam with a special insertion probe (Figure 1 and Table 3).

4. STEAM CHEMISTRY

Steam in Italian fields has variable chloride contents depending on the depth and position of the geothermal reservoir. This experimental study has been conducted on steam with chloride contents between 0 and 35 ppm, to cover the normal concentration range present in the exploited steam.

In each measurement the steam composition was analyzed at the start and end of each test. Table 3 shows the chemical-physical features of the utilized steam.

5. EXPERIMENTAL DESCRIPTION

Inserting the corrosion coupons into direct contact with steam performed the experiments. The coupons were cooled by

internally circulating water to allow vapour to condense on the sample surface and generate a localised dew point.

5.1 Experimental Apparatus

A retractable probe was used to expose samples to steam. The probe could be inserted and removed from pipeline during flowing conditions. This was done with a special stuffing box (Figure 1) and a pressure relief valve (Figure 2) that was attached to the pipeline through a ball valve (size 1", pressure rating 5 MPa).

The cylindrically shaped corrosion samples were hollow to allow cooling water to circulate. They had a 20 cm^2 surface area (Figure 3).

Sample cooling was obtained with a closed refrigerating loop (Figure 4). The cooling water was stored in a 10 m^3 tank and was pumped into the probe by a centrifugal pump. The water was discharged through a pipe coaxially positioned in relation to the inlet water pipe. The hot water from the probe was then cooled with a heat exchanger cooled by air fluxed with a fan.

Cold and warm water temperatures in the test system were continuously measured by "J type" thermocouples connected to a chart recorder. Water flow rates in the cooling system were measured by direct volumetric change.

5.2 Experimental Protocol

Each sample was marked and weighed at the beginning of each test and then inserted in the steam. Sample cooling was obtained by circulating water in the probe core at a flow rate of about 0.25 m^3/h. In steady conditions, the difference between entering water (≈ 35 °C) and the outlet water was about 22°C (Figure 5). Samples were exposed to steam for 7 days and the steam was sampled and analysed at the start and the end of each run.

Sample polishing was performed according to ASTM G 1 recommendations. Evaluation of corrosion damage was performed according to the same protocols for general corrosion evaluation and according to ASTM G 46 protocols for pitting corrosion.

6. EXPERIMENTAL RESULTS

Several tests were performed in superheated steam having different chloride concentrations to find a correlation between chloride content and corrosion rate in the zones where steam begins to condense.

All cured coupons showed a preferential attack on the surface exposed to steam impact. API 5LX carbon steel was mainly affected by general corrosion, as expected (Figure 6). AISI 403 exhibited negligible general corrosion but significant pitting damage (Figure 7).

The experimental data showed good repeatability (Tables 4 and 5). The corrosion rate on carbon steel rises with the increasing of chloride concentration in the dry superheated steam. Acceptable corrosion rate has been measured only with low chloride concentrations (about 0.2 mm/yr with 0.5 ppm), while with few ppm of chlorides it was too severe (about 2.8 mm/yr with 9 ppm). This confirms a chloride induced corrosion mechanism due to the presence of a very acid condensate on the metal surface. A significant concentration of chloride has been found in the corrosion products, confirming the acid mechanism of the attack.

Experimental corrosion rates on carbon steel are in agreement with field data in Larderello area (less than 0.3 mm/yr in dry superheated steam with low chloride content and more than 5 mm/yr with steam containing more than 20 ppm of chloride) and in Krafla, Iceland (Hirtz et al. 1991).

AISI 403 stainless steel has not showed severe general corrosion rate (less than 0.25 mm/yr till to 9.2 ppm), but many pits with an average depth of 20 micron resulted after only 7 days of exposure. This phenomenon agrees with field experiences in Larderello (Italy) and in Krafla (Iceland) areas, where severe corrosion of turbine components, mostly at the base of stationary and moving 13% chromium steel blades in the wet stages of the machines, was monitored.

The results show an empirical correlation between the carbon steel corrosion rate and chloride content in the steam (Figure 8), as expressed in [1].

$$Corr.rate = 0{,}315 \cdot [Cl]_{steam} \qquad [1]$$

where *Corr. Rate* is in mm/yr and [Cl] in ppm.

7. CONCLUSIONS

Direct corrosion rate measurements in superheated steam at chloride contents between 0.5 and 9 ppm have allowed characterization of the aggressiveness of some of Italian geothermal fluids exploited for power production. Experimental and field data were in a very good agreement.

The adopted experimental method can be used as a good way to predict the corrosion rate in wet zones of pipelines and turbines, where superheated steam occurs.

The empirical relationship between the corrosion rate and chloride content can be used as a tool for the assessment of the material in the design and operation of pipelines and turbines. It also allows a determination of the empirical limits for chloride contents requiring the adoption of chloride abatement plants.

REFERENCES

Bracaloni, M., Culivicchi, G., and Fornari B. (1995). Erosion and corrosion problems experienced during the operation of geothermal turbines in Italy. *Proc. World Geothermal Congress 1995*, Vol. 4, pp. 2427 – 2432.

Allegrini, G., and Benvenuti, G. (1970). Corrosion characteristics and geothermal power plant protection (collateral processes of abrasion, erosion and scaling). *Geothermics*, Special Issue 9, Part I, pp. 865 – 881.

Viviani, E., Paglianti, A., Sabatelli, F., and Tarquini, B. (1995). Abatement of hydrogen chloride in geothermal power plants. *Proc. World Geothermal Congress 1995*, Vol. 4, pp. 2421 – 2426.

Hirtz, P., Buck, C., and Kunzman, R. (1991). Current techniques in acid-chloride corrosion control and monitoring at the Geysers. *Proc. Sixteenth Workshop on Geothermal Reservoir Engineering Standford University, Standford, California, January 23-25*

ASTM G1 *Preparing, cleaning and evaluating corrosion test specimens.*

ASTM G46 *Examination and evaluation of pitting corrosion.*

Table 1: Modeling results on Lumiera well

Parameter	Super-heated steam	Dew-Point composition	
		Constant pressure cooling	Adiabatic expansion
Temp. [°C]	240	184	137
Pressure [Mpa]	1.1	1.1	0.35
pH	5.4	3.8	3.9
CO_2 [ppm]	17,000	30.2	9.3
H_2S [ppm]	450	2.5	0.9
H_3BO_3 [ppm]	476	41,800	118,800
HCl [ppm]	21	0.9	1.4
NH_3 [ppm]	39	5.2	3.8
HCO_3^- [ppm]	-	0.03	0.03
HS^- [ppm]	-	0.002	0.002
$CO_3^=$ [ppm]	-	Traces	Traces
$S^=$ [ppm]	-	Traces	Traces
$H_2BO_3^-$ [ppm]	-	0.3	1.6
Cl^- [ppm]	-	2800	10,800
NH_4^+ [ppm]	-	1400	5500
Boiling point [°C] elevation.	-	1.2	2.8

Table 2 Chemical composition of steels

API 5LX	C	S	P	Mn
	0.29 max	0.05 max	0.04 max	1.25 max
	Si	Cr	Ni	Mo
	-	-	-	-
AISI 403	C	S	P	Mn
	0.6 – 0.15	0.03 max	0.03 max	0.25 – 0.80
	Si	Cr	Ni	Mo
	0.05 max	11.25 - 13	0.5 max	0.30 max

Table 3 Chemical composition and thermodynamic properties of steam

		Ciabattino well	Gabbro pipeline	Farinello Pipeline		Puntone 1 well
				1	2	
Flow rate	(kg/h)	7100	138,000	383,000	405,000	34,500
Press.	(bar)	5.7	6.9	5.2	5.0	3.4
T	(°C)	154	225	212	211	245
NCG	(%v)	9.9	8.4	7.3	6.1	-
pH		6.25	5.85	5.10	5.70	6.15
Alc.	(meq HCl/l)	22.1	8.3	4.72	-	4.2
NH_4^+	(ppm)	247	-	132	-	102.3
Cl^-	(ppm)	0.54	2.9	9.2	3.7	32.4
H_3BO_3	(ppm)	23.3	193	246	-	211
H_2S	(ppm)	60.3	36.5	45.5	-	-

Table 4 Corrosion results on API 5LX carbon steel

Chloride conc. [ppm]	Corrosion rate	
	[mg/cm^2 year]	[mm/year]
0.54	149	0.19
	180	0.23
2.4	547	0.7
2.9	625	0.8
	797	1
	911	1.2
3.7	1068	1.36
	1080	1.38
9.2	2155	2.7
	2200	2.8
	2200	2.8
32.4	3990	5.1
	4145	5.3

Table 5 Corrosion rates on AISI 403 stainless steel

Chloride content [ppm]	Corrosion rate		Pitting density [ASTM G46]	Average pitting depth [µm]
	[mg/cm^2·yr]	[mm/yr]		
2.9	152	0.19	5 10^5/m^2	21
	144	0.18	5 10^5/m^2	20
9.2	172	0.22	5 10^5/m^2	26
	187	0.24	5 10^5/m^2	27

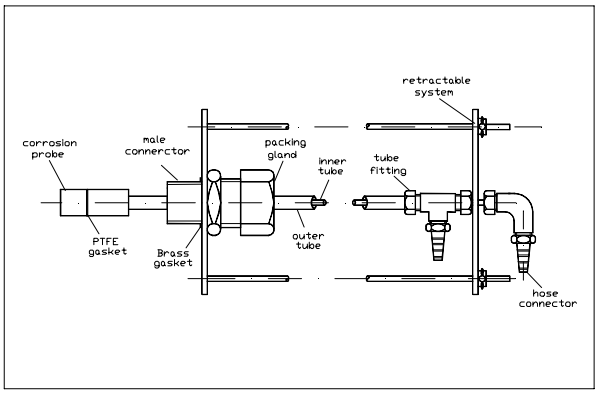

Figure 1 Insertion probe and sample holder

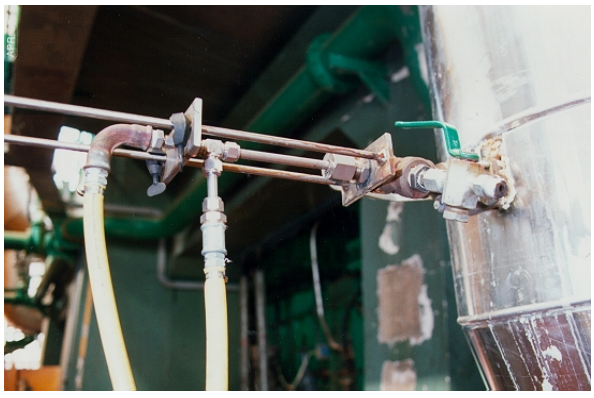

Figure 2 Probe inserted in the pipeline

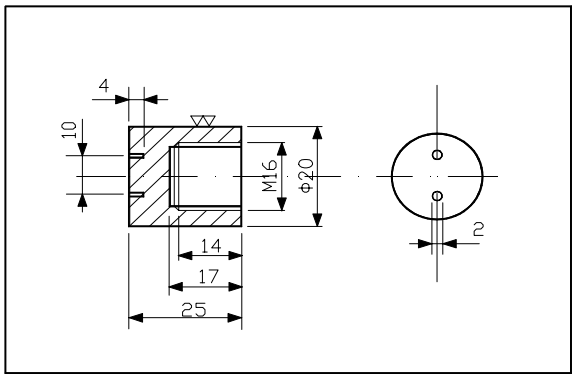

Figure 3 Corrosion coupon design

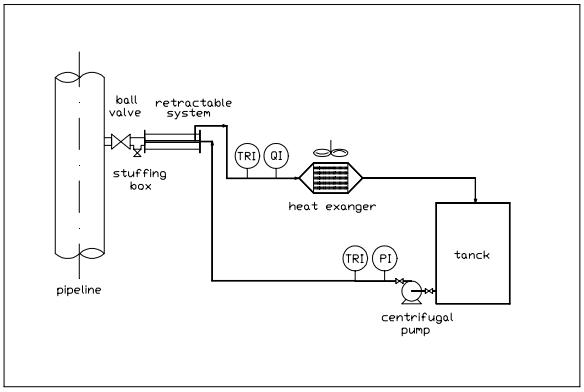

Figure 4 Test loop configuration

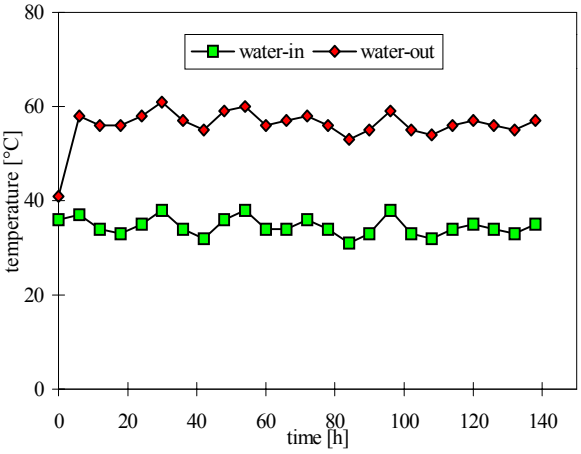

Figure 5 Cooling water temperatures

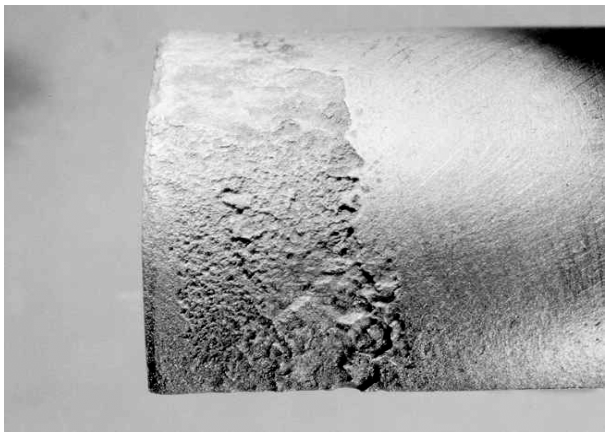

Figure 6 API 5LX after 9.2 ppm Cl exposure

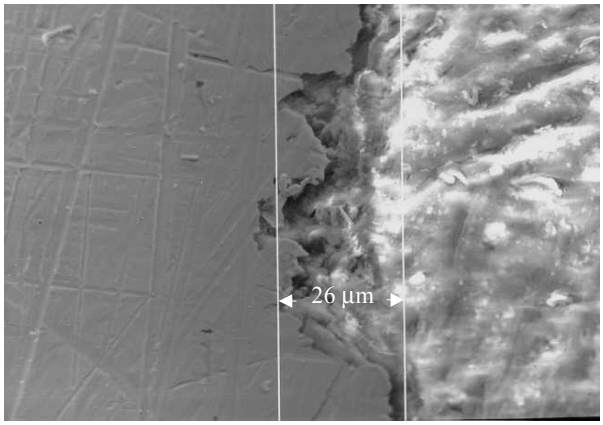

Figure 7 AISI 403 – average depth of pitting damage

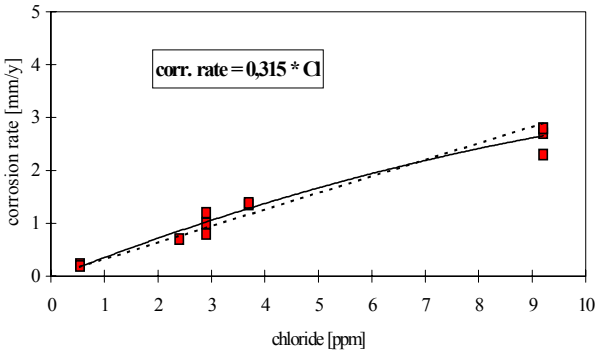

Figure 8 Corrosion rate vs chloride concentration